ISSN 2229-5518

The Effect of Secondary Flow on Heat Transfer from a Rotating Sphere to Oldroyd-B Fluid

S. E. E. Hamza

Abstract— The subject of this work is the study of the effect of secondary flow on heat transfer from a rotating sphere to Oldroyd-B fluid. The Navier-Stokes equations governing the steady axisymmetric flow can be written as two coupled, nonlinear partial differential equations for the stream function and rotational velocity component. Slow flow approximation is used to solve the equations of motion and the energy equation. Therefore, all dynamical variables in the governing equations are expanded in power series in terms of Reynolds number *Re*, and Deborah number *De*. The solution of the obtained partial differential equations is valid for small values of *Re* and *De*, and all values of Prandtl number *Pr*. The analysis of the obtained solution shows that, the stream function consists of two additional secondary flow parts caused by elastic and inertia effects. So, the properties of the resultant stream line pattern depend on the relative magnitudes of the two parts. If *Re* and *De* differ from each other appreciably, then one is dominant and imprints its character on what happens. Under certain conditions, the superposition leads to a different situation. At some critical values of *Re* and *De* it is noticed that, a spherically shaped stagnation stream surface is formed in the fluid. The radius of this surface is calculated. The effect of the secondary flow on the temperature distribution and heat transfer rate are calculated and analyzed. Flow patterns of velocity distribution, temperature profile and Nusselt number are presented at $Pr = 0.7$ and for different values of *Re* and *De*.

Index Terms— Heat transfer, Oldroyd-B, Prandtl number, Rotating sphere, Secondary flow, Stagnation surface, Stream function.

1 Introduction

THE problem of rotating sphere in viscoelastic fluid and the associated problem of heat transfer have been studied extensively by several rheologests due to its importance in various technical and rheological problems. Examples of these problems are rotary machines, spherical heat exchangers and rheological measurements of the viscoelastic fluids parameters. Also, the secondary flow field which occurs around the rotating sphere have an important influence in chemical engineering (e.g., mixing processes) and dynamics of separation processes [1], [2], [3], [4], [5], [6], [7]. Reiner [8] was the first who formulate the rheological equation of state of a fluid for which normal stresses occur in steady shear flow, and Weissenberg [9] actually demonstrated the presence of such effect. Ericksen alone [10] and in collaboration with Rivilin [11] pointed out that, under certain conditions such normal stresses may lead to secondary flow phenomena.

Giesekus [12] has solved and applied experimentally the problem of a rotating sphere in a second-order viscoelastic fluid up to the first-order approximation by using the perturbation method. The obtained secondary flow pattern is equivalent to our first-order solution one only. Giesekus carried out the experiment using a sphere of 48 mm. diameter which rotates in a 5% aqueous solution of Polyacrylamide at $22\ ^{o}C$. The main result of this experiment is that, the normal stresses produce a secondary flow towards the sphere in the equatorial plane and away from it along the axis of rotation. But with increasing the angular velocity, the streamlines of the secondary flow shift slightly towards the pole axis and at some critical speeds a zone of double torus divided by the equatorial plane is formed. Giesekus observed this effect experimentally and he pointed out (without theoretical interpretation) that it depends on the fluid properties and on the angular velocity of the sphere.

In fact, the fluid parameters such as viscosity, first normal stress and second normal stress are very sensitive to temperature changes. Moreover, the fluid suffering from a large temperature variation in industry due to forced mechanical operations. This application increases the gap between the measured parameters in laboratory and real parameters control the motion in industry. Hence, the temperature is considered as a source of error in rheological measurements. So, the aim of the present work is to deduce the effect of secondary flow on heat transfer with application of an external temperature source on the sphere boundary. This helps us to improve the control of the fluid motion in applications [13].

Free convection from a rotating sphere has been investigated by many researchers. Taking into account the extra terms of O(*Re*) in the velocity field predicted by Proudmann and Pearson [14], Rimmer [15], [16] obtained an improved expression for the mean Nusselt number describing the rate of heat transfer from the solid surface. His results are in good agreement with the numerical results of Dennis et al. [17]. Takhar and Whitelaw [18] extended this study to the case of a rotating sphere taking the velocity field given by Whitelaw [19]. They observed that rotation enhances heat transfer.

The problem of interest in the current study involves the effect of secondary flow due to elastic and inertia on the velocity and temperature fields around a rotating sphere in viscoelastic fluid. We use an approximate method for the limit of small Reynolds and Deborah numbers. This method is quite reasonable and is satisfied in many practical situations. The results of the secondary flow, stream lines and torque predict the experimental results qualitatively [12] and can be applied to the upper-convected Maxwell fluid and Newtonian fluids.

• *Salah Eed Ebrahim Hamza, Physics Department, Faculty of Science, Benha University, Egypt, PH-00201122688273, E-mail: salah.hamza@fsc.bu.edu.eg*

ISSN 2229-5518

2 Governing Equations

We consider a uniformly heated sphere of radius R rotates in an infinite viscoelastic fluid media with an angular velocity Ω about its polar axis. Spherical polar coordinate system $(\tilde{r},\theta,\varphi)$ with its origin at the center of the sphere and the line $\theta=0$ as the polar axis is adopted to describe the mathematical formulation, Fig. 1. It is assumed that, the sphere is kept at constant temperature $\tilde{T}_1$, while the fluid is still maintained at $\tilde{T}_2$ with $\tilde{T}_1>\tilde{T}_2$. The fluid has a density ρ, heat capacity per unit mass c_p, and thermal conductivity k.

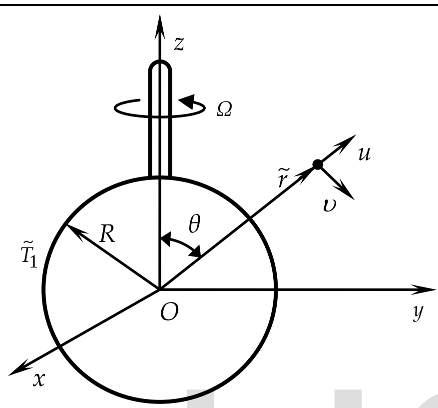

Fig. 1. Flow geometry.

The equations governing steady, incompressible, and viscoelastic flow are continuity, momentum, and energy equations

$$\tilde{\nabla}\cdot\underline{v}=0, \tag{1a}$$

$$\rho\left(\underline{v}\cdot\tilde{\nabla}\underline{v}\right)=-\tilde{\nabla}p+\tilde{\nabla}\cdot\underline{\underline{\tilde{\tau}}}, \tag{1b}$$

$$\rho\, c_p\,\underline{v}\cdot\tilde{\nabla}\tilde{T}=k\tilde{\nabla}^2\tilde{T}, \tag{1c}$$

here $\underline{v}$ is the velocity vector, p is the pressure, $\tilde{T}$ is the temperature of the fluid and $\underline{\underline{\tilde{\tau}}}$ is the stress tensor which is given from Oldroyd-B model [20], [21] as:

$$\underline{\underline{\tilde{\tau}}}+\lambda_1\overset{\nabla}{\underline{\underline{\tilde{\tau}}}}=2\eta_o\left(\underline{\underline{\tilde{d}}}+\lambda_2\overset{\nabla}{\underline{\underline{\tilde{d}}}}\right), \tag{2}$$

where $\underline{\underline{\tilde{d}}}$ is the rate of strain tensor, λ_1 is the relaxation time, λ_2 is the retardation time, η_o is the zero-shear rate viscosity and the symbol "∇" over any tensor denotes the upper-convected derivative. Setting $\lambda_2=0$ in (2) reduces it to Maxwell model while Newtonian fluid is obtained by setting $\lambda_1=\lambda_2=0$.

In spherical polar coordinates, the velocity field and the temperature may be written as:

$$\underline{v}=\left[u(\tilde{r},\theta),\ \upsilon(\tilde{r},\theta),\ w(\tilde{r},\theta)\right],\quad \tilde{T}=\tilde{T}(\tilde{r},\theta), \tag{3}$$

the velocity and the temperature are independent of the coordinate φ due to the symmetry about the z-axis. Since the flow is described in the meridian plane, the velocity components u and υ can be expressed in terms of the stream function $\psi(\tilde{r},\theta)$, which satisfy the continuity equation as:

$$\underline{v}_{\perp}=u\hat{\tilde{r}}+\upsilon\hat{\theta}=\left(\frac{-\psi_{,\theta}}{\tilde{r}^2\sin\theta}\right)\hat{\tilde{r}}+\left(\frac{\psi_{,r}}{\tilde{r}\sin\theta}\right)\hat{\theta}=-\tilde{\nabla}\wedge\left(\frac{\psi}{\tilde{r}\sin\theta}\hat{\varphi}\right). \tag{4}$$

Taking the divergence of (2) then substituting in (1b), we get

$$\rho\left(\underline{v}\cdot\tilde{\nabla}\underline{v}\right)=-\tilde{\nabla}p+2\eta_o\tilde{\nabla}\cdot\underline{\underline{\tilde{d}}}-\tilde{\nabla}\cdot\left(\lambda_1\overset{\nabla}{\underline{\underline{\tilde{\tau}}}}-2\eta_o\lambda_2\overset{\nabla}{\underline{\underline{\tilde{d}}}}\right). \tag{5}$$

Let the radius of the sphere, R, and the angular velocity, Ω, be reference values of length and velocity, respectively. Then nondimensional variables can be defined via:

$$\left.\begin{aligned}&r=\frac{\tilde{r}}{R},\ \nabla=R\tilde{\nabla},\ \Psi=\frac{\psi}{R^3\Omega},\ \underline{V}=\frac{\underline{v}}{R\Omega},\ P=\frac{p}{\eta_o\Omega},\\&\underline{\underline{\tau}}=\frac{\underline{\underline{\tilde{\tau}}}}{\eta_o\Omega},\ \overset{\nabla}{\underline{\underline{\tau}}}=\frac{\overset{\nabla}{\underline{\underline{\tilde{\tau}}}}}{\eta_o\Omega^2},\ \underline{\underline{d}}=\frac{\underline{\underline{\tilde{d}}}}{\Omega},\ \overset{\nabla}{\underline{\underline{d}}}=\frac{\overset{\nabla}{\underline{\underline{\tilde{d}}}}}{\Omega^2},\ T=\frac{\tilde{T}-\tilde{T}_2}{\tilde{T}_1-\tilde{T}_2}.\end{aligned}\right\} \tag{6}$$

Introducing the above dimensionless quantities into (2), (4), (5) and (1c), we get

$$\underline{\underline{\tau}}=2\underline{\underline{d}}-De\left(\overset{\nabla}{\underline{\underline{\tau}}}-2\xi\overset{\nabla}{\underline{\underline{d}}}\right), \tag{7a}$$

$$\underline{V}_{\perp}=U\hat{r}+V\hat{\theta}=-\nabla\wedge\left(\frac{\Psi}{r\sin\theta}\hat{\varphi}\right), \tag{7b}$$

$$\nabla^2\underline{V}-Re\,\underline{\Gamma}-De\,\underline{\Lambda}-\nabla P=0, \tag{7c}$$

$$Pr\,Re\,\underline{V}\cdot\nabla T=\nabla^2 T, \tag{7d}$$

where the two vectors $\underline{\Gamma}$ and $\underline{\Lambda}$ are given by:

$$\underline{\Gamma}=\underline{V}\cdot\nabla\underline{V}, \tag{8a}$$

$$\underline{\Lambda}=\nabla\cdot\left(\overset{\nabla}{\underline{\underline{\tau}}}-2\xi\overset{\nabla}{\underline{\underline{d}}}\right). \tag{8b}$$

and $\xi=\dfrac{\lambda_2}{\lambda_1}$. Equations (7) are characterized by Deborah number De, Reynolds number Re and Prandtl number Pr given by:

$$De=\lambda_1\Omega,\qquad Re=\frac{\rho R^2\Omega}{\eta_o},\qquad Pr=\frac{c_p\eta_o}{k}. \tag{9}$$

Since $\underline{V}=\underline{V}_{\perp}+W\hat{\varphi}$, $\underline{\Gamma}=\underline{\Gamma}_{\perp}+\Gamma_3\hat{\varphi}$ and $\underline{\Lambda}=\underline{\Lambda}_{\perp}+\Lambda_3\hat{\varphi}$ with $\underline{V}_{\perp}=U\hat{r}+V\hat{\theta}$, $\underline{\Gamma}_{\perp}=\Gamma_1\hat{r}+\Gamma_2\hat{\theta}$ and $\underline{\Lambda}_{\perp}=\Lambda_1\hat{r}+\Lambda_2\hat{\theta}$, then (7c) may be decomposed into the φ-component and the vector equation including the r- and θ-components as:

$$\nabla^2\left(W\hat{\varphi}\right)-\left(Re\,\Gamma_3+De\,\Lambda_3\right)\hat{\varphi}=0, \tag{10a}$$

$$\nabla^2\underline{V}_{\perp}-Re\,\underline{\Gamma}_{\perp}-De\,\underline{\Lambda}_{\perp}-\nabla P=0. \tag{10b}$$

Applying the curl operation to (10b) and using (7b), the equations of motion, (10a) and (10b), after some mathematical handling are reduced to:

$$\frac{1}{r^2}\left\{\partial_r\left(r^2W_{,r}\right)+\partial_\theta\left[\frac{1}{\sin\theta}\partial_\theta\left(W\sin\theta\right)\right]\right\}-Re\,\Gamma_3-De\Lambda_3=0 \tag{11a}$$

$$\left[\partial_r^2+\frac{\sin\theta}{r^2}\,\partial_\theta\left(\frac{1}{\sin\theta}\partial_\theta\right)\right]^2\Psi-Re\,\sin\theta\left[\partial_r\left(r\Gamma_2\right)-\partial_\theta\Gamma_1\right]-De\,\sin\theta\left[\partial_r\left(r\Lambda_2\right)-\partial_\theta\Lambda_1\right]=0 \tag{11b}$$

The components of $\underline{\Gamma}$ and $\underline{\Lambda}$ are given in the Appendix.

ISSN 2229-5518

3 Boundary Conditions

We assume that, the sphere is kept at constant temperature $\tilde{T}_1$ while the fluid at infinity is still at $\tilde{T}_2$ such that $\tilde{T}_1 > \tilde{T}_2$. Also we assume that, the sphere is rotating with angular velocity $\underline{\Omega} = \Omega\,\hat{z}$. The linear velocity at infinity vanishes, $\underline{v}(\infty) = 0$, while at the sphere surface is $\underline{v}(R) = \underline{\Omega} \wedge R\,\hat{\tilde{r}} = \Omega\, R \sin\theta\, \hat{\varphi}$. Therefore, the boundary conditions in dimensionless form may be formulated as:

$$W = \begin{Bmatrix} \sin\theta \\ 0 \end{Bmatrix},\ \Psi = \Psi_{,r} = \begin{Bmatrix} 0 \\ 0 \end{Bmatrix},\ T = \begin{Bmatrix} 1 \\ 0 \end{Bmatrix} \text{ for } r = \begin{Bmatrix} 1 \\ \infty \end{Bmatrix}, \tag{12a}$$

and the symmetry conditions at the poles, $(\theta = 0,\ \pi)$, are:

$$W = \Psi = \Psi_{,r} = T = \begin{Bmatrix} 0 \\ 0 \end{Bmatrix} \quad \text{for} \quad \theta = \begin{Bmatrix} 0 \\ \pi \end{Bmatrix}. \tag{12b}$$

4 The Method of Successive Approximation

The solution of the problem is obtained by the perturbation method. The perturbation parameters that describe the importance of the inertial and elastic effects are the Reynolds and Deborah numbers. So, the dynamical variables are expanded as a power series in *Re* and *De*. For example, for *H* we write

$$H = \sum_{m,n=0} Re^m\, De^n\, H^{(m,n)} = H^{(0,0)} + Re\,H^{(1,0)} + De H^{(0,1)} + Re\,De\,H^{(1,1)} + \ \ldots \tag{13}$$

with the help of (13), the governing equations, (7a), (11a) and (11b) take the form:

$$\sum_{m,n=0} Re^m\, De^n \left[\underline{\underline{\tau}}^{(m,n)} - 2\underline{\underline{d}}^{(m,n)} + De\left(\overset{\nabla}{\underline{\underline{\tau}}}{}^{(m,n)} - 2\xi\, \overset{\nabla}{\underline{\underline{d}}}{}^{(m,n)} \right) \right] = 0 \tag{14a}$$

$$\sum_{m,n=0} Re^m\, De^n \left\{ \frac{1}{r^2}\left[\partial_r\left(r^2 W_{,r}^{(m,n)}\right) + \partial_\theta\left(\frac{1}{\sin\theta}\partial_\theta\left(W^{(m,n)} \sin\theta\right)\right)\right] - Re\,\Gamma_3^{(m,n)} - De\,\Lambda_3^{(m,n)} \right\} = 0, \tag{14b}$$

$$\sum_{m,n=0} Re^m\, De^n \left\{ \left[\partial_r^2 + \frac{\sin\theta}{r^2}\partial_\theta\left(\frac{1}{\sin\theta}\partial_\theta\right)\right]^2 \Psi^{(m,n)} - Re\,\sin\theta\left[\partial_r\left(r\Gamma_2^{(m,n)}\right) - \partial_\theta \Gamma_1^{(m,n)}\right] - De\,\sin\theta\left[\partial_r\left(r\Lambda_2^{(m,n)}\right) - \partial_\theta\Lambda_1^{(m,n)}\right] \right\} = 0. \tag{14c}$$

The boundary conditions, (12a), can be written as:

$$W^{(m,n)} = \begin{Bmatrix} \delta_{m0}\delta_{0n}\sin\theta \\ 0 \end{Bmatrix},\ \Psi^{(m,n)} = \Psi_{,r}^{(m,n)} = \begin{Bmatrix} 0 \\ 0 \end{Bmatrix},$$

$$T^{(m,n)} = \begin{Bmatrix} \delta_{m0}\delta_{0n} \\ 0 \end{Bmatrix},\ \text{ for } r = \begin{Bmatrix} 1 \\ \infty \end{Bmatrix}. \tag{14d}$$

where δ_{ij} is the Kronecker delta function.

5 Solution of the Flow Equations

The solution of (7d) and (14) subject to the boundary conditions (14d) up to the first order, is the chief object of this paper. The flow equations are not coupled with the energy equation and need to be solved before the solution of the later one.

5.1 Creeping Flow

This step of approximation produces the leading terms in the expansion of *W*, Ψ and *T*. The solution of these terms represent the creeping flow around the rotating sphere [22]. The lowest order in (14) are:

$$\underline{\underline{\tau}}^{(0,0)} = 2\underline{\underline{d}}^{(0,0)}, \tag{15a}$$

$$\partial_r\left(r^2 W_{,r}^{(0,0)}\right) + \partial_\theta\left(\frac{1}{\sin\theta}\partial_\theta\left(W^{(0,0)}\sin\theta\right)\right) = 0, \tag{15b}$$

$$\left[\partial_r^2 + \frac{\sin\theta}{r^2}\ \partial_\theta\left(\frac{1}{\sin\theta}\partial_\theta\right)\right]^2 \Psi^{(0,0)} = 0, \tag{15c}$$

with the boundary conditions:

$$W^{(0,0)} = \sin\theta,\ 0 \text{ and } \Psi^{(0,0)} = \Psi_{,r}^{(0,0)} = 0,\ 0 \text{ for } r = 1,\ \infty. \tag{15d}$$

The solutions of (15b) and (15c) which satisfies the boundary conditions are:

$$W^{(0,0)} = \frac{\sin\theta}{r^2}, \tag{16a}$$

and

$$\Psi^{(0,0)} = 0. \tag{16b}$$

Regarding the heat transfer prediction, the coefficient of $Re^0\, De^0$ in the energy equation, (7d), shows that the function $T^{(0,\,0)}$ must satisfy the equatioin:

$$\nabla^2 T^{(0,0)} = 0, \tag{17a}$$

or

$$r^2 T_{,rr}^{(0,0)} + 2rT_{,r}^{(0,0)} + T_{,\theta\theta}^{(0,0)} + \cot\theta\, T_{,\theta}^{(0,0)} = 0, \tag{17b}$$

with the boundary conditions:

$$T^{(0,0)} = 1,\ 0 \quad \text{for} \quad r = 1,\ \infty. \tag{17c}$$

The solution of (17b) and (17c) is:

$$T^{(0,0)} = \frac{1}{r}. \tag{17d}$$

5.2 Secondary Flow due to Inertial Effect

In this section, we find the secondary flow due to small inertial effects (centrifugal forces). Therefore, the coefficients of $Re^1\, De^0$ in (14) are:

$$\frac{1}{r^2}\left[\partial_r\left(r^2 W_{,r}^{(1,0)}\right) + \partial_\theta\left(\frac{1}{\sin\theta}\partial_\theta\left(W^{(1,0)}\sin\theta\right)\right)\right] - \Gamma_3^{(0,0)} = 0, \tag{18a}$$

$$\left[\partial_r^2 + \frac{\sin\theta}{r^2}\partial_\theta\left(\frac{1}{\sin\theta}\partial_\theta\right)\right]^2 \Psi^{(1,0)} - \sin\theta\left[\partial_r\left(r\Gamma_2^{(0,0)}\right) - \partial_\theta\Gamma_1^{(0,0)}\right] = 0, \tag{18b}$$

with

$$W^{(1,0)} = 0,\ 0 \text{ and } \Psi^{(1,0)} = \Psi_{,r}^{(1,0)} = 0,\ 0 \text{ for } r = 1,\ \infty. \tag{18c}$$

The solution of (18) requires the determination of $\Gamma_i^{(0,0)}$ for $i = 1,2,3$. Since $\underline{V}^{(0,0)} = \left[0,\ 0,\ W^{(0,0)}\right]$, we get from (A.1) in the Appendix the components $\Gamma_i^{(0,0)}$ as:

$$\Gamma_1^{(0,0)} = U^{(0,0)}U_{,r}^{(0,0)} + \frac{1}{r}\left(V^{(0,0)}U_{,\theta}^{(0,0)} - V^{(0,0)2} - W^{(0,0)2}\right) = -r^{-5}\sin^2\theta, \tag{19a}$$

$$\Gamma_2^{(0,0)} = U^{(0,0)}V_{,r}^{(0,0)} + \frac{1}{r}\left(V^{(0,0)}V_{,\theta}^{(0,0)} + U^{(0,0)}V^{(0,0)}\right),$$

$$-W^{(0,0)2}\cot\theta\Big) = -r^{-5}\sin\theta\cos\theta\,, \tag{19b}$$

and

$$\Gamma_3^{(0,0)} = U^{(0,0)}W,_r^{(0,0)} + \frac{1}{r}\Big(V^{(0,0)}W,_\theta^{(0,0)} + U^{(0,0)}W^{(0,0)} + V^{(0,0)}W^{(0,0)}\cot\theta\Big) = 0\,. \tag{19c}$$

Therefore, (18) take the forms:

$$\partial_r\left(r^2W,_r^{(1,0)}\right) + \partial_\theta\left(\frac{1}{\sin\theta}\partial_\theta\left(W^{(1,0)}\sin\theta\right)\right) = 0\,, \tag{20a}$$

$$\left[\partial_r^2 + \frac{\sin\theta}{r^2}\partial_\theta\left(\frac{1}{\sin\theta}\partial_\theta\right)\right]^2\Psi^{(1,0)} = 6r^{-5}\sin^2\theta\cos\theta\,. \tag{20b}$$

The boundary conditions imposed on (20) implies that, the only solution satisfying (20a) is:

$$W^{(1,0)} = 0\,, \tag{21a}$$

and the solution of (20b) is:

$$\Psi^{(1,0)} = \frac{1}{8}\left(1 - \frac{1}{r}\right)^2 \sin^2\theta\ \cos\theta\,. \tag{21b}$$

By taking (7b) into account, the components of the velocity $\underline{V}_\perp^{(1,0)}$ can be calculated from $\Psi^{(1,0)}$ as:

$$U^{(1,0)} = \frac{-1}{r^2\sin\theta}\Psi,_\theta^{(1,0)} = \frac{1}{8}r^{-4}(r-1)^2\left(1 - 3\cos^2\theta\right), \tag{21c}$$

and

$$V^{(1,0)} = \frac{1}{r\sin\theta}\Psi,_r^{(1,0)} = \frac{1}{4}r^{-4}(r-1)\ \sin\theta\cos\theta\,. \tag{21d}$$

5.3 Secondary Flow due to Elastic Effect

The coefficients of $Re^0\, De^1$ in (14) are

$$\underline{\underline{\tau}}^{(0,1)} = 2\underline{\underline{d}}^{(0,1)} - \overset{\nabla(0,0)}{\underline{\underline{\tau}}} + 2\xi\overset{\nabla(0,0)}{\underline{\underline{d}}} \tag{22a}$$

$$\frac{1}{r^2}\left[\partial_r\left(r^2W,_r^{(0,1)}\right) + \partial_\theta\left(\frac{1}{\sin\theta}\partial_\theta\left(W^{(0,1)}\sin\theta\right)\right)\right] - \Lambda_3^{(0,0)} = 0 \tag{22b}$$

$$\left[\partial_r^2 + \frac{\sin\theta}{r^2}\partial_\theta\left(\frac{1}{\sin\theta}\partial_\theta\right)\right]^2\Psi^{(0,1)} - \sin\theta\left[\partial_r\left(r\Lambda_2^{(0,0)}\right) - \partial_\theta\Lambda_1^{(0,0)}\right] = 0 \tag{22c}$$

with the boundary conditions

$$W^{(0,1)} = 0,\ 0 \ \text{and}\ \Psi^{(0,1)} = \Psi,_r^{(0,1)} = 0,\ 0\ \text{for}\quad r = 1,\ \infty\,. \tag{22d}$$

The lowest order solution shows that, the non-vanishing components of $\underline{\underline{\tau}}^{(0,0)}$ and $\underline{\underline{d}}^{(0,0)}$ are:

$$\tau_{r\varphi}^{(0,0)} = 2d_{r\varphi}^{(0,0)} = \frac{1}{r}\left(rW,_r^{(0,0)} - W^{(0,0)}\right) = -3r^{-3}\sin\theta \tag{23a}$$

therefore, by using (A.4) and (A.5), the non-vanishing components of $\overset{\nabla(0,0)}{\underline{\underline{\tau}}}$ and $\overset{\nabla(0,0)}{\underline{\underline{d}}}$ are:

$$\overset{\nabla(0,0)}{\tau}_{\varphi\varphi} = 2\overset{\nabla(0,0)}{d}_{\varphi\varphi} = -18r^{-6}\sin^2\theta \tag{23b}$$

while any other components are zeros. Therefore, the components of the vector $\underline{\Lambda}^{(0,0)}$ appearing in (22) are given by:

$$\Lambda_1^{(0,0)} = 18(1-\xi)\, r^{-7}\ \sin^2\theta\,, \tag{24a}$$

$$\Lambda_2^{(0,0)} = 18(1-\xi)\, r^{-7}\ \sin\theta\cos\theta\,, \tag{24b}$$

and

$$\Lambda_3^{(0,0)} = 0\,. \tag{24c}$$

Since $\Lambda_3^{(0,0)} = 0$, then the only solution of (22b) is the identical solution:

$$W^{(0,1)} = 0\,. \tag{25}$$

Equation (22c), after substitution of $\Lambda_1^{(0,0)}$ and $\Lambda_2^{(0,0)}$, reduces to:

$$\left[\partial_r^2 + \frac{\sin\theta}{r^2}\partial_\theta\left(\frac{1}{\sin\theta}\partial_\theta\right)\right]^2\Psi^{(0,1)} = -144(1-\xi)r^{-7}\sin^2\theta\cos\theta\,, \tag{26a}$$

the solution of this equation for the boundary conditions (22d) is:

$$\Psi^{(0,1)} = -\frac{1}{2}(1-\xi)r^{-3}(r-1)^2(r+2)\sin^2\theta\cos\theta\,. \tag{26b}$$

From $\Psi^{(0,1)}$ we can obtain the components of the velocity $\underline{V}_\perp^{(0,1)}$ as:

$$U^{(0,1)} = \frac{-1}{r^2\sin\theta}\Psi,_\theta^{(0,1)} = -\frac{1}{2}(1-\xi)r^{-5}(r-1)^2(r+2)\left(1 - 3\cos^2\theta\right), \tag{26c}$$

$$V^{(0,1)} = \frac{1}{r\sin\theta}\Psi,_r^{(0,1)} = -3(1-\xi)r^{-5}(r-1)\sin\theta\ \cos\theta\,, \tag{26d}$$

6 Effects Of Secondary Flow On Heat Transfer

Energy equation, (7d), is a non-linear second-order partial differential equation. The density function, $\underline{V}\cdot\nabla T$, in its left hand side is known from the solution of the flow equations. The secondary flow effects on heat transfer through its contribution to the velocity field. To find these effects due to both inertia and elastic, we solve the energy equation up to the second-order approximation.

6.1 Inertial Effects

The coefficient of $Re^1\, De^0$ in (7d) is:

$$\nabla^2 T^{(1,0)} = Pr\,\underline{V}^{(0,0)}\cdot\nabla T^{(0,0)}\,, \tag{27a}$$

with the boundary conditions

$$T^{(1,0)} = 0\,,\ 0 \quad \text{for} \quad r = 1,\ \infty\,. \tag{27b}$$

By taking the zero-order solution into account, the right hand side of (27a) equal to zero. So, the solution of (27a) with the boundary conditions (27b) is:

$$T^{(1,0)} = 0\,. \tag{27c}$$

The coefficient of $Re^2\, De^0$ in (7d) is:

$$\nabla^2 T^{(2,0)} = Pr\left[\underline{V}^{(0,0)}\cdot\nabla T^{(1,0)} + \underline{V}^{(1,0)}\cdot\nabla T^{(0,0)}\right]\,, \tag{28a}$$

with the boundary conditions

$$T^{(2,0)} = 0\,,\ 0 \quad \text{for} \quad r = 1,\ \infty\,. \tag{28b}$$

The right hand side of (28a) can be calculated as:

$$\underline{V}^{(0,0)}\cdot\nabla T^{(1,0)} = 0\,, \tag{28c}$$

$$\underline{V}^{(1,0)}\cdot\nabla T^{(0,0)} = U^{(1,0)}T,_r^{(0,0)} = -\frac{1}{8}r^{-6}(r-1)^2\left(1 - 3\cos^2\theta\right), \tag{28d}$$

therefore, (28a) takes the form:

$$\left[\partial_r\left(r^2\partial_r\right) + \frac{1}{\sin\theta}\partial_\theta\left(\sin\theta\ \partial_\theta\right)\right]T^{(2,0)} = -\frac{1}{8}Pr\ r^{-4}(r-1)^2\left(1 - 3\cos^2\theta\right) \tag{29a}$$

the complete solution of the last equation is:

$$T^{(2,0)}=\frac{1}{96}Pr\,(r-1)\left(3r^{-3}+2r^{-4}\right)\left(1-3\cos^2\theta\right). \quad (29b)$$

6.2 Elastic Effect

To show the elastic effect on heat transfer due to normal stresses, we solve the energy equation up to the first order of $Re\,De$. So, the coefficient of this order in (7d) is:

$$\nabla^2 T^{(1,1)}=Pr\left(\underline{V}^{(0,0)}\cdot\nabla T^{(0,1)}+\underline{V}^{(0,1)}\cdot\nabla T^{(0,0)}\right), \quad (30a)$$

with the boundary conditions

$$T^{(1,1)}=0\,,\ 0 \qquad \text{for} \qquad r=1,\ \infty\,. \quad (30b)$$

By using (17d) and (26), the terms in the right hand side of (30a) are given by:

$$\underline{V}^{(0,0)}\cdot\nabla T^{(0,1)}=0\,, \quad (31a)$$

$$\underline{V}^{(0,1)}\cdot\nabla T^{(0,0)}=U^{(0,1)}T,_r^{(0,0)}=\frac{1}{2}(1-\xi)\,r^{-7}(r-1)^2(r+2)\left(1-3\cos^2\theta\right) \quad (31b)$$

so, (30a) takes the form:

$$\left[\partial_r\left(r^2\partial_r\right)+\frac{1}{\sin\theta}\partial_\theta\left(\sin\theta\ \partial_\theta\right)\right]T^{(1,1)}=\frac{1}{2}Pr(1-\xi)\,r^{-5}(r-1)^2(r+2)\left(1-3\cos^2\theta\right) \quad (32a)$$

the solution of this equation is:

$$T^{(1,1)}=-\frac{1}{56}Pr(1-\xi)(r-1)\left(7r^{-3}-10r^{-4}+4r^{-5}\right)\left(1-3\cos^2\theta\right). \quad (32b)$$

7 RESULTS AND DISCUSSION

7.1 Streamline and Velocity Profiles

According to the perturbation technique employed in section (4), the solution of the boundary value problem defined by (14c) is being:

$$\Psi(r,\theta)=Re\,\Psi^{(1,0)}+De\,\Psi^{(0,1)}\,, \quad (33a)$$

which shows that, the effective secondary flow of a viscoelastic fluid results from the superposition of both inertia, $\Psi^{(1,0)}$, and elastic, $\Psi^{(0,1)}$, components. The different signs of the expressions in (21b) and (26b) show in fact that both effects have opposing tendencies in respect of the flow direction. Therefore, the properties of the resultant streamline pattern depend on the relative magnitudes of the two effects, or more accurately, on the ratio of *Re* to *De*. By using (21b) and (26b), it is possible to obtain the stream function in dimensionless form as:

$$\Psi=A\left[1-B\left(1+\frac{2}{r}\right)\right]\left(1-\frac{1}{r}\right)^2\sin^2\theta\,\cos\theta\,, \quad (33b)$$

where

$$A=\tfrac{1}{8}Re \qquad \text{and} \qquad B=\frac{4\,De\,(1-\xi)}{Re}. \quad (33c)$$

From the definition of the stream function, (4), and by using (33b), it is possible to obtain the individual velocity components U and V as:

$$U=\frac{-1}{r^2\sin\theta}\Psi,_\theta=\frac{A}{r^2}\left[1-B\left(1+\frac{2}{r}\right)\right]\left(1-\frac{1}{r}\right)^2\left(1-3\cos^2\theta\right), \quad (34a)$$

and

$$V=\frac{1}{r\sin\theta}\Psi,_r=\frac{2A}{r^3}\left(1-\frac{3B}{r}\right)\left(1-\frac{1}{r}\right)\ \sin\theta\cos\theta\,. \quad (34b)$$

The known expressions for the velocity components must be introduced in the expression of $\underline{V}$ to obtain the complete solution for the velocity field around the rotating sphere as:

$$\underline{V}=U\hat{r}+V\hat{\theta}+W^{(0)}\hat{\varphi}\,, \quad (35)$$

As expected, the stream and velocity functions show that the flow field is under the effect of both inertial and elastic effects. The dimensionless quantity "B" in (33b) determines the shape of the streamline and velocity profiles while "A" determines their absolute values. Secondary flow is a consequence of interaction between both inertial and elastic forces. The flow pattern varies with the value of "B" as the following:

1. For $B\le\frac{1}{3}$, the inertial force determines the nature of flow field as in Figs. 2a, 3a and 4a. These forces caused fluid to be thrown outward centrifugally at equatorial zone. So, the secondary flow is directed to the inside at the poles ($\theta=0,\pi$) and to the outside at the equator zone ($\theta=\frac{1}{2}\pi$).
2. For $\frac{1}{3}<B<1$, the elastic forces dominate near the surface of the sphere and further away from the sphere, the inertial forces dominate the flow situation. A complete picture of such flow situation is given in Figs. 2b, 3b and 4b.
3. For $B\ge 1$, the secondary flow due to elastic forces is dominate, see Figs. 2c, 3c and 4c. It is directed to the inside in the equator zone and to the outside at the poles. The two zones being separated by conical surface given by $\theta_{min}=\cos^{-1}\sqrt{\frac{1}{3}}\cong 54.75^o$. This behavior is in agreement with the flow pattern observed experimentally [12].
4. For $B>2$, the shape of the streamline and velocity profile become independent on B, see Figs. 2d, 3d and 4d.

The primary flow, meridunal velocity $W^{(0)}$ in Fig. 5a, is a pure drag flow for which every fluid point revolves in a circle whose center lies on the axis of rotation. All particles that rotate with the same angular velocity lie on one surface of rotation. So, the flow field consists of a set of rotational symmetric layers, which rotate at various angular velocities around the common axis. So, the adjacent layers slide over each other and there is an overall shear flow that results from the zero-order stress component $\tau_{r\varphi}^{(0,0)}$, (23a). Fig. 5b shows that, $\tau_{r\varphi}^{(0,0)}$ reaches its maximum value on the equator zone ($\theta=\frac{1}{2}\pi$) and vanishes at the poles ($\theta=0,\pi$). For shear flow, it is well known that the normal stress differences are proportional to the square of the shear rate [21]. Therefore, the fluid under the action of this normal stress difference flows inwards in the vicinity of the equator (high stress difference) and outwards at the poles (low stress difference).

ISSN 2229-5518

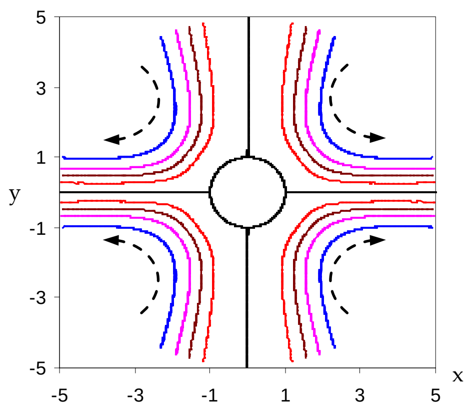

Fig. 2a. Stream lines at $B = 0.3$. Inertial force caused fluid to be thrown outward centrifugally at the equatorial zone.

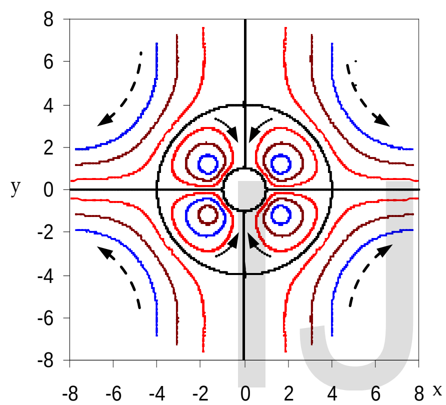

Fig. 2b. Stream lines at $B = 0.66$. Elastic forces dominate near the sphere surface and inertial forces dominate away from the sphere

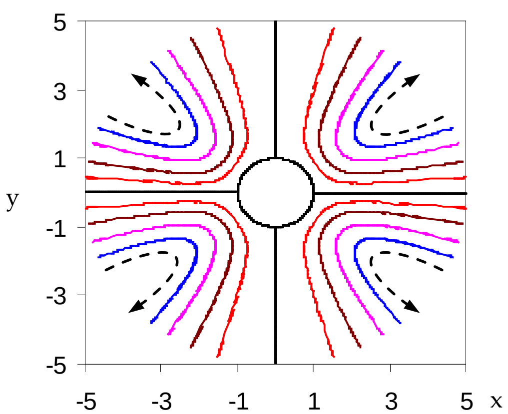

Fig. 2c. Stream lines $B = 2$. Elastic force caused fluid to be thrown inward at equator zone.

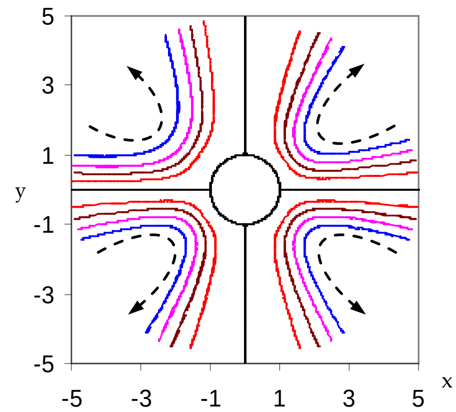

Fig. 2d. Stream lines at $B = 3$. For $B > 2$, the shape of the streamline become independent on B.

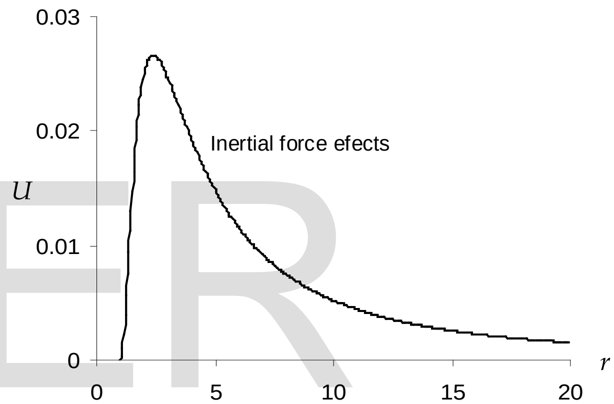

Fig. 3a. Radial velocity at $B = 0.3,\ \theta = \pi/2$. For $B < 1/3$, the inertial forces determine the nature of the radial velocity profiles.

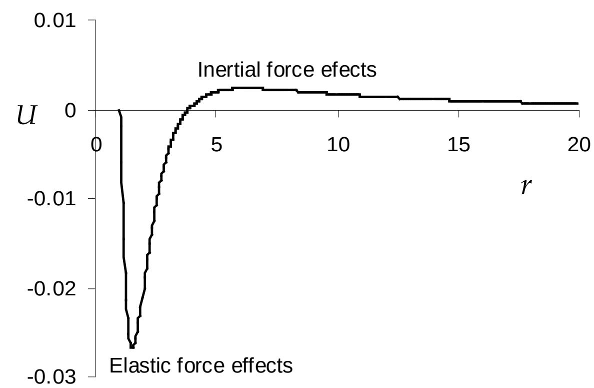

Fig. 3b. Radial velocity at $B = 0.66,\ \theta = \pi/2$. For $1/3 < B < 1$, elastic forces dominate near the sphere surface and inertial forces dominate away from the sphere.

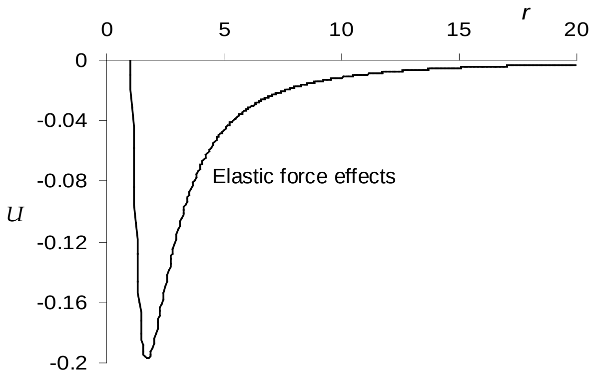

Fig. 3c. Radial velocity at $B = 2,\ \theta = \pi/2$. For $B \geq 1$, elastic forces determine the nature of the radial velocity profiles.

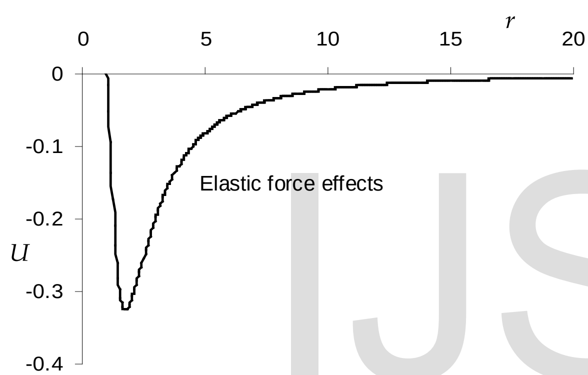

Fig. 3d. Radial velocity at $B = 3,\ \theta = \pi/2$. For $B > 2$, the shape of the velocity profiles become independent on B.

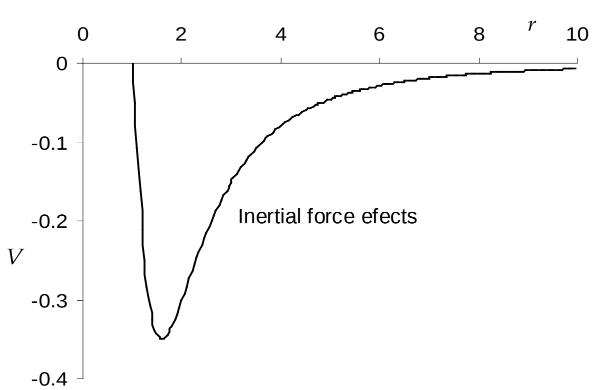

Fig. 4a. Azimuthal velocity at $B = 0.3,\ \theta = \pi/2$. For $B < 1/3$, the inertial forces determine the nature of the velocity profiles.

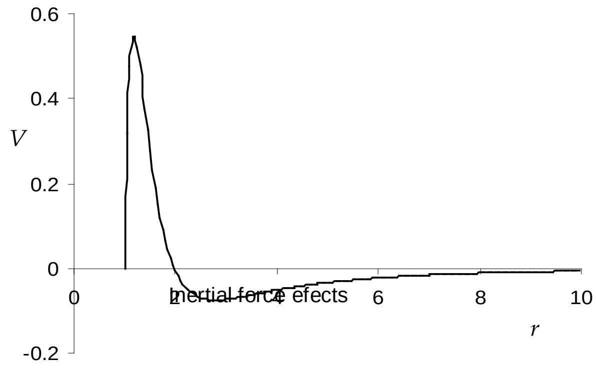

Fig. 4b. Azimuthal velocity at $B = 0.66,\ \theta = \pi/2$. For $1/3 < B < 1$, elastic forces dominate near the sphere surface and inertial forces dominate away from the sphere

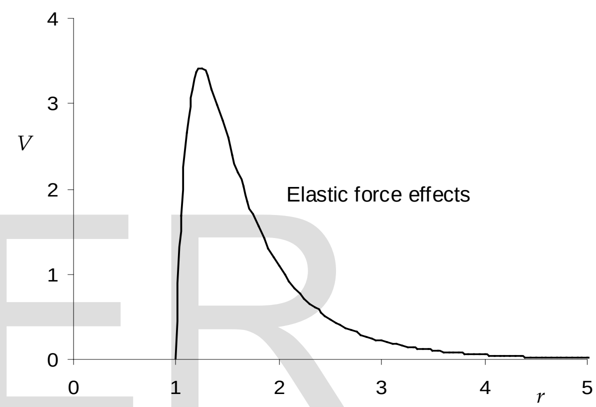

Fig. 4c. Azimuthal velocity at $B = 2,\ \theta = \pi/2$. For $B \geq 1$, elastic forces determine the nature of the azimuthal velocity profiles.

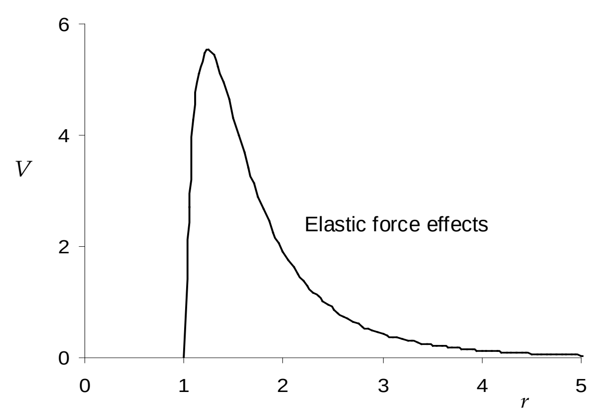

Fig. 4d. Azimuthal velocity at $B = 3,\ \theta = \pi/2$. For $B > 2$, the shape of the velocity profiles become independent on B.

Elastic force effects

ISSN 2229-5518

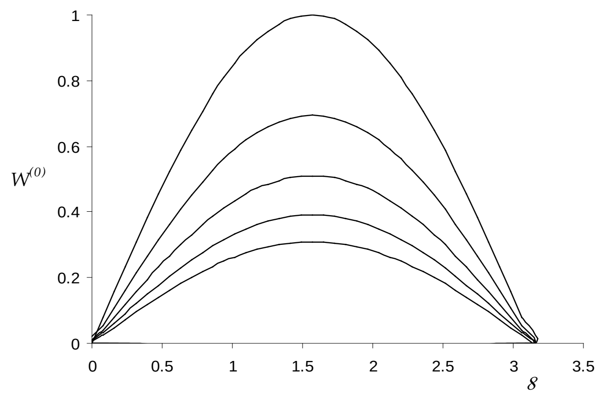

Fig. 5a. Meridunal velocity $W^{(0)}$ at $B=2$, and $r=1, 1.2, 1.4, 1.6, 1.8$ (top to bottom respectively)

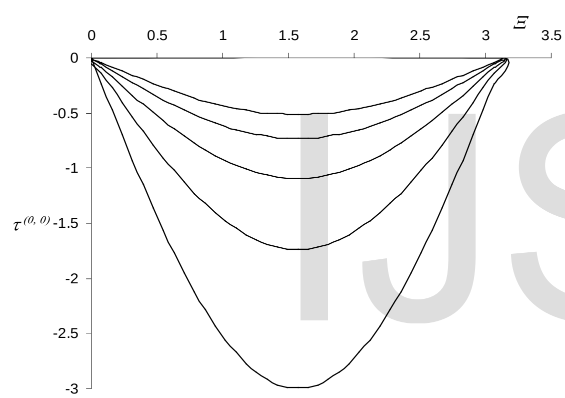

Fig. 5b. Stress tensor component $\tau_{r\varphi}^{(0,0)}$ at $B=2$, and $r=1, 1.2, 1.4, 1.6, 1.8$ (bottom to top respectively)

7.2 Stagnation Stream Surface

It is clear that, the properties of the resultant stream line pattern depend on the numerical value of the parameter B. From (9) and (33c), we can write the parameter B as:

$$B=\frac{4(\lambda_1-\lambda_2)\eta_o}{\rho R^2}. \tag{36}$$

Note that this parameter apart from the physical properties (ρ, η_o, λ_1 and λ_2), depends only on radius of the sphere R, but not on its rate of rotation. Therefore, for a given viscoelastic fluid, the flow pattern can only be affected by the size of the rotating sphere.

If the parameter $B=B_o$ where B_o has its value between $\frac{1}{3}$ and one ($\frac{1}{3}<B_o<1$) which can always be obtained by a suitable sized sphere, then a spherically shaped stagnation stream surface occurs in the fluid. As shown in Fig. 2b; the stream line of the normalized stream function $\Psi(r,\theta)$ divides the annular region between the rotating sphere and the stagnation surface into four similar vortices symmetric about the axis of rotation. The elastic stress effect is dominant inside, so that the same direction results as shown in Fig. 2b. The externally prevailing inertia effect causes the outer vortices to rotate in the opposite direction.

The stagnation sphere of radius R_o is defined as the surface for which $U=0$. So by using (34a) we can calculate the value of R_o as:

$$R_o=\frac{2B_o}{1-B_o}. \tag{37}$$

The effect of the stagnation surface on heat transfer process is discussed in more details in later section.

7.3 Eddy Points

The eddy points, or secondary flow centers, are defined as the points for which $U=V=0$. From (34a) and (34b) these points are given by:

$$\left[1-B\left(1+\frac{2}{r}\right)\right]\left(1-\frac{1}{r}\right)^2\left(1-3\cos^2\theta\right)=0, \tag{38a}$$

and

$$\left(1-\frac{3B}{r}\right)\left(1-\frac{1}{r}\right)\sin\theta\,\cos\theta=0, \tag{38b}$$

Equation (38a) gives the radius R_o of the stagnation surface. Fig. 6 shows that, the eddy points are formed in the interior of the fluid between $1<r<R_o$. So, it may be calculated from (38a) and (38b) that, if an eddy point exists, it may lie either on $\theta_{min}=\cos^{-1}\sqrt{1/3}\cong 54.75^o$, $1-3\cos^2\theta=0$, or on a circular streamline $r=R_c=3B_o$ for which $V=0$, see the red circle in Fig. 6. So, the coordinates of any eddy is $(3B_o,\ 54.74^o)$.

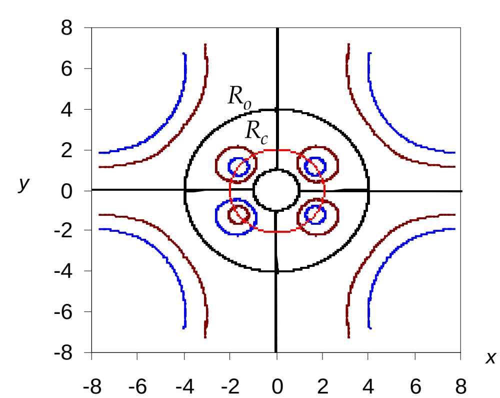

Fig. 6. Stagnation stream surface and eddy points

From the temperature point of view, the circular streamline of radius $R_c=3B_o$ divides the annular region between the solid sphere, $r=1$, and the stagnation surface, $r=R_o$, into two concentric parts. The inner region in the range $1<r<R_c$ represents a temperature suction region in which the rotating

eddy absorb the temperature from the heated solid sphere and then inject it to the outer region in the range $R_c < r < R_o$.

7.4 Heat Transfer Results

As we have seen in the previous sections, the flow depends on *Re* and *De* while the temperature distribution depends on *Re*, *De* and *Pr*. The solution of the energy equation is given by:

$$T = T^{(0,0)} + Re^2\, T^{(2,0)} + Re\, De\, T^{(1,1)}. \tag{39a}$$

The zero- and the higher-orders solution of the energy equation are given by (17d), (29b) and (32b) respectively. So, the resultant temperature is given by:

$$T = r^{-1} + \frac{2}{21} A^2\, Pr\,(r-1)\Big[7\big(3r^{-3} + 2r^{-4}\big) - 3B\big(7r^{-3} - 10r^{-4} + 4r^{-5}\big)\Big]\big(1 - 3\cos^2\theta\big) \tag{39b}$$

In this study, it is more convenient to work in terms of the local Nusselt number, *Nu*, which can be obtained from the gradient of the temperature at the surface of the sphere and at the stagnation surface:

$$Nu_1 = T_{,r}\big|_{r=1} = -1 + A^2\, Pr(35 - 3B)\big(1 - 3\cos^2\theta\big), \tag{40a}$$

$$Nu_2 = T_{,r}\big|_{r=R_0} = \big(1 - 3\cos^2\theta\big), \tag{40b}$$

Figs. 7a and 7b show the local hemispheric Nusselt number distributions for the solid sphere and the stagnation surface (Nu_1, Nu_2) respectively at $B = 0.66$, and $A = 0.1$. At the equator, cold fluid was pulled from the stagnation surface to the solid sphere, and heat transfer from the solid sphere was at its greatest. Therefore, there was a local maximum for the Nu_1 distribution. Afterwards, fluid moving up and down to the poles along the fluid was heated gradually by the hot wall. Meanwhile, the temperature gradient in the radial direction and Nu_1 decreased gradually forms a local Nu_1 minimum at the poles. By contrast, at the poles, where the stagnation sphere received heat from the hot radial outflow, heat transfer at the stagnation sphere was at its greatest, thereby forming a local maximum at Nu_2 distribution. Fluid returning to the equator along the stagnation sphere was then cooled gradually by the cold fluid. Meanwhile, the temperature gradient in the radial direction and Nu_2 decreased gradually forms local minimal of Nu_2 at the equator.

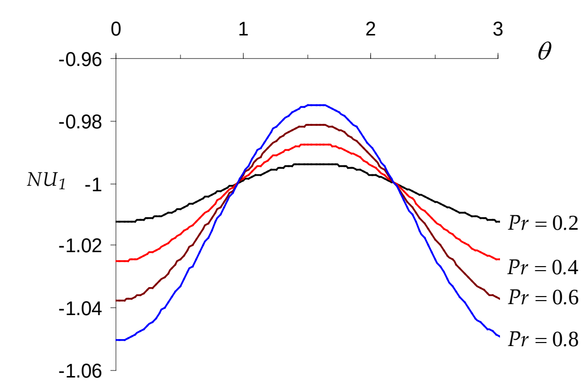

Fig. 7a. Nusselt number distributions for the solid sphere $r = 1$ at $B = 0.66$, $A = 0.1$ and different values of *Pr*.

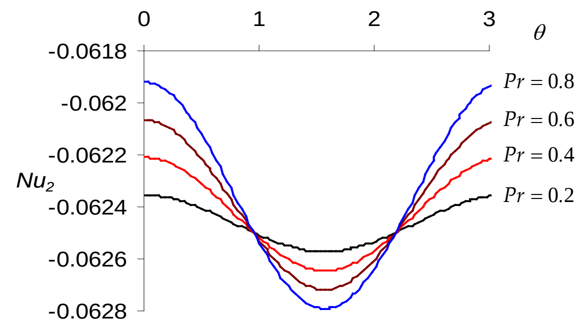

Fig. 7b. Nusselt number distributions for stagnation surface $r = R_o$ at $B = 0.66$, $A = 0.1$ and different values of *Pr*.

8 CONCLUSION

The problem to be treated here is the study of the secondary flow effect on heat transfer from a rotating sphere to Oldroyd-B fluid. With the help of the perturbation method, the governing equations are splitted into two parts: creeping part, and the deviation describing the disturbance due to inertia and elastic effects. The solution of the problem shows that, any rotation of the sphere set up a primary flow around the axis of rotation. This motion induces an unbalanced inertial and elastic force fields which drives the secondary flow in the meridian plane. The secondary flow produces forced convection within the fluid. The relative magnitudes of the secondary flow and forced convection effects depend on the parameters involved such as Reynolds, Deborah and Prandtl numbers.

9 Estimation of the Error Due to the Shaft

In the absence of the shaft, the slow rotation of the sphere about the z-axis is supposed to create a laminar velocity field whose magnitude at the surface of the sphere is:

$$W\big|_{\tilde{r}=R} = \Omega R \sin\theta\ , \tag{41}$$

the shear stress due to this component, at the surface can be estimated as:

$$\tau\big|_{\tilde{r}=R} = \eta_o W_{,\tilde{r}}\big|_{\tilde{r}=R} = \eta_o\, \Omega \sin\theta\,. \tag{42}$$

The power required to overcome this stress in order to rotate the sphere is approximately

$$P_W = \int_0^{2\pi} d\varphi \int_0^{\pi} [\tau\, W]_{\tilde{r}=R}\, R^2 \sin\theta\, d\theta = \tfrac{8}{3}\pi\eta_o \Omega^2 R^3\,. \tag{43}$$

This power is responsible for the torque acting on the sphere surface.

In the presence of a cylindrical shaft, an additional velocity field is created due to its rotation. The tangential velocity component of this field in the neighborhood of its surface is:

$$\overset{*}{W} = \Omega R_s\,, \tag{44}$$

where R_s is the radius of the shaft, see Fig. 8. Similarly, the stress created by this field requires an amount of power to rotate the shaft. This power is of magnitude

$$\overset{*}{P}_W = \int_0^{2\pi} d\varphi \int_0^{L_s} [\overset{*}{\tau}\,\overset{*}{W}]_{\tilde{r}=R_s} R^2 \sin\theta \; d\theta = 2\pi\eta_o\Omega^2 R_s^2 L_s \; . \tag{45}$$

The error caused by the shaft can be estimated as the ratio

$$\frac{\overset{*}{P}_W}{P_W} = \frac{3R_s^2 L_s}{4R^3} \; . \tag{46}$$

Thus, using a shaft of much smaller radius than R may reduce this error. For example, let the radius of the sphere be $R = 2.4Cm$. If the radius of the shaft is 0.16 Cm, and its length (under the fluid surface) is $L_s = 0.5Cm$, then

$$\frac{\overset{*}{P}_W}{P_W} = \frac{3(0.16)^2\,(0.5)}{4(2.4)^3} \le 6.94\times 10^{-4} \, . \tag{47}$$

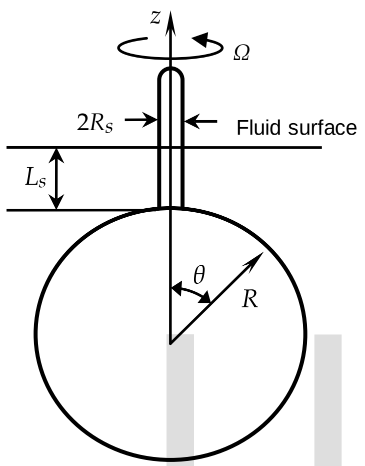

Fig. 8. Error due to the shaft

10 APPENIX

The components of the two vectors $\underline{\Gamma}$ and $\underline{\Lambda}$ defined by (8a) and (8b) are given by the following equations:

(i) Components of $\underline{\Gamma}$

$$\underline{\Gamma} = \underline{V}\cdot\nabla\underline{V} = \Gamma_1\hat{r} + \Gamma_2\hat{\theta} + \Gamma_3\hat{\varphi} \, , \tag{A.1}$$

where

$$\Gamma_1 = \hat{r}\cdot\underline{\Gamma} = UU,_r + \frac{1}{r}\left(VU,_\theta - V^2 - W^2\right),$$

$$\Gamma_2 = \hat{\theta}\cdot\underline{\Gamma} = UV,_r + \frac{1}{r}\left(VV,_\theta + UV - W^2\cot\theta\right),$$

$$\Gamma_3 = \hat{\varphi}\cdot\underline{\Gamma} = UW,_r + \frac{1}{r}\left(VW,_\theta + UW + VW\cot\theta\right).$$

(ii) Components of $\underline{\Lambda}$

$$\underline{\Lambda} = \nabla\cdot\left(\overset{\nabla}{\underline{\underline{\tau}}} - 2\xi\overset{\nabla}{\underline{\underline{d}}}\right) = \Lambda_1\hat{r} + \Lambda_2\hat{\theta} + \Lambda_3\hat{\varphi} \, , \tag{A.2}$$

where

$$\Lambda_1 = \frac{1}{r^2}\partial_r\left[r^2\left(\overset{\nabla}{\tau}_{rr} - 2\xi\overset{\nabla}{d}_{rr}\right)\right] + \frac{1}{r\sin\theta}\partial_\theta\left[\sin\theta\left(\overset{\nabla}{\tau}_{r\theta} - 2\xi\overset{\nabla}{d}_{r\theta}\right)\right] - \frac{1}{r}\left[\left(\overset{\nabla}{\tau}_{\theta\theta} + \overset{\nabla}{\tau}_{\varphi\varphi}\right) - 2\xi\left(\overset{\nabla}{d}_{\theta\theta} + \overset{\nabla}{d}_{\varphi\varphi}\right)\right]$$

$$\Lambda_2 = \frac{1}{r^3}\partial_r\left[r^3\left(\overset{\nabla}{\tau}_{r\theta} - 2\xi\overset{\nabla}{d}_{r\theta}\right)\right] + \frac{1}{r\sin\theta}\partial_\theta\left[\sin\theta\left(\overset{\nabla}{\tau}_{\theta\theta} - 2\xi\overset{\nabla}{d}_{\theta\theta}\right)\right] - \frac{\cot\theta}{r}\left[\overset{\nabla}{\tau}_{\varphi\varphi} - 2\xi\overset{\nabla}{d}_{\varphi\varphi}\right]$$

$$\Lambda_3 = \frac{1}{r^3}\partial_r\left[r^3\left(\overset{\nabla}{\tau}_{r\varphi} - 2\xi\overset{\nabla}{d}_{r\varphi}\right)\right] + \frac{1}{r\sin^2\theta}\partial_\theta\left[\sin^2\theta\left(\overset{\nabla}{\tau}_{\theta\varphi} - 2\xi\overset{\nabla}{d}_{\theta\varphi}\right)\right].$$

The components of the tensors $\underline{\underline{d}}$, $\overset{\nabla}{\underline{\underline{d}}}$ and $\overset{\nabla}{\underline{\underline{\tau}}}$ which are needed for calculating the components of the vector $\underline{\Lambda}$ are:

(i) Components of $\underline{\underline{d}}$ (A.3)

$$d_{rr} = U,_r \; ,$$

$$d_{\theta\theta} = \frac{1}{r}\left(U + V,_\theta\right),$$

$$d_{\varphi\varphi} = \frac{1}{r}\left(U + V\cot\theta\right),$$

$$d_{r\theta} = d_{\theta r} = \frac{1}{2r}\left(U,_\theta + rV,_r - V\right),$$

$$d_{r\varphi} = d_{\varphi r} = \frac{1}{2r}\left(rW,_r - W\right),$$

$$d_{\theta\varphi} = d_{\varphi\theta} = \frac{1}{2r}\left(W,_\theta - W\cot\theta\right).$$

(ii) Components of $\overset{\nabla}{\underline{\underline{d}}}$ (A.4)

$$\overset{\nabla}{d}_{rr} = Ud_{rr,r} + r^{-1}Vd_{rr,\theta} - 2d_{rr}d_{rr} - 2r^{-1}U,_\theta d_{r\theta} \, ,$$

$$\overset{\nabla}{d}_{\theta\theta} = Ud_{\theta\theta,r} + r^{-1}Vd_{\theta\theta,\theta} - 2d_{\theta\theta}d_{\theta\theta} - 2r^{-1}(rV,_r - V)d_{r\theta} \, ,$$

$$\overset{\nabla}{d}_{\varphi\varphi} = Ud_{\varphi\varphi,r} + r^{-1}Vd_{\varphi\varphi,\theta} - 2d_{\varphi\varphi}d_{\varphi\varphi} - 4d_{r\varphi}d_{r\varphi} - 4d_{\theta\varphi}d_{\theta\varphi} \, ,$$

$$\overset{\nabla}{d}_{r\theta} = Ud_{r\theta,r} + r^{-1}Vd_{r\theta,\theta} + d_{\varphi\varphi}d_{r\theta} - r^{-1}(rV,_r - V)d_{rr} - r^{-1}U,_\theta d_{\theta\theta} \, ,$$

$$\overset{\nabla}{d}_{r\varphi} = Ud_{r\varphi,r} + r^{-1}Vd_{r\varphi,\theta} + d_{\theta\theta}d_{r\varphi} - 2d_{r\varphi}d_{rr} - 2d_{\theta\varphi}d_{r\theta} - r^{-1}U,_\theta d_{\theta\varphi} \, ,$$

$$\overset{\nabla}{d}_{\theta\varphi} = Ud_{\theta\varphi,r} + r^{-1}Vd_{\theta\varphi,\theta} + d_{rr}d_{\theta\varphi} - 2d_{\theta\varphi}d_{\theta\theta} - 2d_{r\varphi}d_{r\theta} - r^{-1}(rV,_r - V)d_{r\varphi} \, .$$

(iii) Components of $\overset{\nabla}{\underline{\underline{\tau}}}$ (A.5)

$$\overset{\nabla}{\tau}_{rr} = U\tau_{rr,r} + r^{-1}V\tau_{rr,\theta} - 2d_{rr}\tau_{rr} - 2r^{-1}U,_\theta \tau_{r\theta} \, ,$$

$$\overset{\nabla}{\tau}_{\theta\theta} = U\tau_{\theta\theta,r} + r^{-1}V\tau_{\theta\theta,\theta} - 2d_{\theta\theta}\tau_{\theta\theta} - 2r^{-1}(rV,_r - V)\tau_{r\theta} \, ,$$

$$\overset{\nabla}{\tau}_{\varphi\varphi} = U\tau_{\varphi\varphi,r} + r^{-1}V\tau_{\varphi\varphi,\theta} - 2d_{\varphi\varphi}\tau_{\varphi\varphi} - 4d_{r\varphi}\tau_{r\varphi} - 4d_{\theta\varphi}\tau_{\theta\varphi} \, ,$$

$$\overset{\nabla}{\tau}_{r\theta} = U\tau_{r\theta,r} + r^{-1}V\tau_{r\theta,\theta} + d_{\varphi\varphi}\tau_{r\theta} - r^{-1}(rV,_r - V)\tau_{rr} - r^{-1}U,_\theta \tau_{\theta\theta} \, ,$$

$$\overset{\nabla}{\tau}_{r\varphi} = U\tau_{r\varphi,r} + r^{-1}V\tau_{r\varphi,\theta} + d_{\theta\theta}\tau_{r\varphi} - 2d_{r\varphi}\tau_{rr} - 2d_{\theta\varphi}\tau_{r\theta} - r^{-1}U,_\theta \tau_{\theta\varphi} \, ,$$

$$\overset{\nabla}{\tau}_{\theta\varphi} = U\tau_{\theta\varphi,r} + r^{-1}V\tau_{\theta\varphi,\theta} + d_{rr}\tau_{\theta\varphi} - 2d_{\theta\varphi}\tau_{\theta\theta} - 2d_{r\varphi}\tau_{r\theta} - r^{-1}(rV,_r - V)\tau_{r\varphi} \, .$$

11 ACKNOWLEDGMENT

The author, S. E. E. Hamza wish to thank Prof. Dr. A. Abou-El Hassan, Prof. of physics, Faculty of Science, Benha University, for his helpful guidance and valuable comments.

12 REFERENCES

[1] M.B. Bush, "The stagnation flow behind a sphere," *J. Non-Newtonian Fluid Mech.*, vol. **49**, no. 1, pp. 103, 1993.

[2] C. Bodart, and M.J. Crochet, "The time-dependent flow of a viscoelastic fluid around a sphere," *J. Non-Newtonian Fluid Mech.*, vol. **54**, pp. 303, 1994.

[3] M.D., Chilcott, and J.M. Rallison, "Creeping flow of dilute polymer solutions past cylinders and spheres," *J. Non-Newtonian Fluid Mech.*, vol. **29**, pp. 381, 1988.

[4] M.T. Arigo, and G.H. McKinley, "The effects of viscoelasticity on the transient motion of a sphere in a shear-thinning fluid," *J. Rheol.*, vol. **41**, no. 1, pp. 103, 1997.

[5] M.T. Arigo, and G.H. McKinley, "An experimental investigation of negative wakes behind spheres settling in shear-thinning viscoelastic fluid," *Rheol. Acta*, vol. **37**, pp. 307, 1998.

[6] E.S. Asmolov, and J.B. McLaughlin, "The internal lift on an oscillating sphere in a linear shear flow," *International J. Muliphase Flow*, vol. **25**, no. 4, pp. 739, 1999.

[7] R.S. Alassar, and H.M. Badr, "Oscillating viscous flow over a sphere," *Computers and Fluids*, vol. **26**, no. 7, pp. 661, 1997.

[8] M. Reiner, *Am. J. Math.*, vol. **67**, pp. 350, 1945.

[9] K. Weissenberg, *Proc. 1st. Intern. Congr. Rheology*, vol. **3**, North Holland Publishing Co., Amsterdam, pp. 36, 1949.

[10] J.L. Ericksen, Quart. Appl. Math., vol. **14**, pp. 318, 1956.

[11] J.L. Ericksen, and R.S. Rivilin, *J. Rat. Math. Anal*. vol. **4**, pp. 323, 1955.

[12] H. Giesekus, "Some secondary flow phenomena in general viscoelastic fluids," *Proceedings of the Fourth International Congress on Rheology*, Wiley-Interscience, New York, vol **1**, pp. 249, 1965.

[13] J.D. Ferry, "*Viscoelastic properties of polymer*," Wiley, New York, 1980.

[14] I. Proudmann, and J.R.A. Pearson, "Expansions at small Reynolds numbers for the flow past a sphere and a circular cylinder," *J. Fluid Mech*. vol. **2**, pp. 237, 1957.

[15] P.L. Rimmer, "Heat transfer from a sphere in a stream of small Reynolds number," *J. Fluid Mech*. vol. **32**, pp. 1, 1968.

[16] P.L. Rimmer, "Heat transfer from a sphere in a stream of small Reynolds number," *Corrigend. J. Fluid Mech*. vol. **35**, no. 4, pp. 827, 1969.

[17] S.C.R. Dennis, J.D.A. Walker and J.D. Hudson, "Heat transfer from a sphere at low Reynolds number," *J. Fluid Mech*. vol. **60**, pp. 273, 1973.

[18] H.S. Takhar and M.H. Whitelaw, "Higher order heat transfer from a rotating sphere," *Acta Mech*. vol. **30**, pp. 101, 1977.

[19] M.H. Whitelaw, "Asymptotic problems in convection and vortices," PhD. Thesis, Manchester Univ., 1974.

[20] R.B. Bird, and J.M. Wiest, "Constitutive equations for polymer liquids," *Annual Rev. Fluid Mech*. vol. **27**, pp. 169-193, 1995.

[21] R.B. Bird, R.C. Armstrong, and O. Hassager, *Dynamics of Polymeric Liquids*, 2nd Edn., vol. **1**, Wiley, New York, 1987.

[22] W.E. Langlois, *Slow viscous flow*, The Macmillan Company, New York, 1964.